Published in final edited form as:
*J Cell Sci*. 2013 January 1; 126(0 1): 60–66. doi:10.1242/jcs.118836.

# Direct mobilisation of lysosomal $Ca^{2+}$ triggers complex $Ca^{2+}$ signals

**Bethan S. Kilpatrick**[1], **Emily R. Eden**[2], **Anthony H. Schapira**[3], **Clare E. Futter**[2], and **Sandip Patel**[1,*]

[1]Department of Cell and Developmental Biology, University College London, London WC1E 6BT, UK

[2]Department of Cell Biology, Institute of Ophthalmology, University College London, London EC1V 9EL, UK

[3]Department of Clinical Neurosciences, Institute of Neurology, University College London, London NW3 2PF, UK

## Summary

Accumulating evidence implicates acidic organelles of the endolysosomal system as mobilisable stores of $Ca^{2+}$ but their relationship to the better-characterised endoplasmic reticulum (ER) $Ca^{2+}$ store remains unclear. Here we show that rapid osmotic permeabilisation of lysosomes evokes prolonged, spatiotemporally complex $Ca^{2+}$ signals in primary cultured human fibroblasts. These $Ca^{2+}$ signals comprised an initial response that correlated with lysosomal disruption and secondary long-lasting spatially heterogeneous $Ca^{2+}$ oscillations that required ER-localised inositol trisphosphate receptors. Electron microscopy identified extensive membrane contact sites between lysosomes and the ER. Mobilisation of lysosomal $Ca^{2+}$ stores is thus sufficient to evoke ER-dependent $Ca^{2+}$ release probably through lysosome-ER membrane contact sites, and akin to the proposed mechanism of action of the $Ca^{2+}$ mobilising messenger nicotinic acid adenine dinucleotide phosphate (NAADP). Our data identify functional and physical association of discrete $Ca^{2+}$ stores important for the genesis of $Ca^{2+}$ signal complexity.

### Keywords

$Ca^{2+}$; Lysosomes; Endoplasmic reticulum; Membrane contact sites; NAADP

## Introduction

Changes in cytosolic $Ca^{2+}$ form the basis of a ubiquitous and highly versatile signalling pathway indispensable for cell function (Berridge et al., 2000). Cytosolic $Ca^{2+}$ signals display marked temporal and spatial heterogeneity in the form of oscillations and waves. They can be confined to a particular subcellular locale or spread through the cell and into neighbouring ones in order to regulate $Ca^{2+}$-dependent targets (Berridge et al., 2000). Many



*Author for correspondence (patel.s@ucl.ac.uk) .



Europe PMC Funders Author Manuscripts

of these signals rely upon the endoplasmic reticulum (ER) which fills with and releases $Ca^{2+}$ through well-defined pumps and channels (Berridge, 2002). $Ca^{2+}$ uptake by mitochondria serves to both shape ER-derived $Ca^{2+}$ signals and to regulate mitochondrial function (Rizzuto et al., 2004). In addition, $Ca^{2+}$ is dynamically regulated by a variety of morphologically eclectic acidic organelles that include the endolysosomal system, lysosome-related organelles, secretory vesicles and the Golgi complex (Patel and Docampo, 2010). Much less is known concerning $Ca^{2+}$ handling by these so called acidic $Ca^{2+}$ stores. This is despite the importance of $Ca^{2+}$ release from endosomes and lysosomes during their fusion (Luzio et al., 2007; Pryor et al., 2000). Indeed, growing evidence links dysfunction of acidic $Ca^{2+}$ stores in lysosomal storage disorders (Lloyd-Evans et al., 2008; Shen et al., 2012), acute pancreatitis (Gerasimenko et al., 2009) and Alzheimer's disease (Coen et al., 2012).

The best characterised route for mobilisation of acidic $Ca^{2+}$ stores is via the potent $Ca^{2+}$ mobilizing messenger nicotinic acid adenine dinucleotide phosphate (NAADP) (Galione et al., 2010). Evidence stems from the use of the lysosomotropic agent GPN (Gly-Phe β-naphthylamide) which causes osmotic permeabilisation of lysosomes through its hydrolysis by the acid hydrolase, cathepsin C (Jadot et al., 1984) resulting in $Ca^{2+}$ depletion. In many cells, GPN selectively blocks NAADP-induced $Ca^{2+}$ release and cytosolic $Ca^{2+}$ signals in response to NAADP-forming agonists (Brailoiu et al., 2006; Churchill et al., 2002; Galione et al., 2010; Yamasaki et al., 2004). NAADP-evoked $Ca^{2+}$ signals are thought to initiate through the activation of the recently described endolysosomal two-pore channels (TPCs) (Brailoiu et al., 2009; Calcraft et al., 2009; Patel et al., 2010; Zong et al., 2009). The resulting release of $Ca^{2+}$ via NAADP has been proposed to 'trigger' further $Ca^{2+}$ release from ER $Ca^{2+}$ stores through inositol trisphosphate ($Ins P_3$) and/or ryanodine receptors (Cancela et al., 1999; Guse and Lee, 2008). 'Chatter' between channels occurs via $Ca^{2+}$-induced $Ca^{2+}$ release (CICR) and/or through the priming of ER $Ca^{2+}$ channels as a result of store overloading (Cancela et al., 1999; Churchill and Galione, 2001; Patel et al., 2001). However, several studies have concluded that NAADP may have more direct effects on the ER through activation of ryanodine receptors (Dammermann et al., 2009; Gerasimenko et al., 2003; Hohenegger et al., 2002). The potential action of NAADP at multiple $Ca^{2+}$ stores, possibly though promiscuous low molecular weight NAADP-binding proteins, has hampered efforts to study the functional relationship between acidic organelles and the ER (Guse, 2012; Lin-Moshier et al., 2012; Marchant et al., 2012). Thus, whether mobilisation of lysosomal $Ca^{2+}$ stores is sufficient to trigger ER $Ca^{2+}$ release is not known.

Recently, we showed that mutation of a dileucine targeting motif in TPC2 (an NAADP-sensitive $Ca^{2+}$-permeable channel) redirects it from its normal lysosomal location to the plasma membrane (Brailoiu et al., 2010). Plasma-membrane-targeted TPC2 was functional as evidenced by both single channel recordings and $Ca^{2+}$ imaging (Brailoiu et al., 2010; Yamaguchi et al., 2011). Importantly, NAADP-evoked $Ca^{2+}$ signals were largely insensitive to blockade of ER $Ca^{2+}$ stores (Brailoiu et al., 2010). Thus, TPCs appeared to be uncoupled from ER $Ca^{2+}$ channels despite being able to mediate global, albeit sluggish, $Ca^{2+}$ increases. These data are indicative of a more intimate relationship between acidic organelles and the ER under normal conditions perhaps akin to membrane contact sites between the ER and the plasma membrane/mitochondria (Patel and Brailoiu, 2012). The latter drive processes such

as excitation-contraction coupling in muscle cells and $Ca^{2+}$ uptake by mitochondria through privileged communication between organelles be it via local $Ca^{2+}$ changes or protein–protein interactions (Protasi, 2002; Rizzuto et al., 2004; Toulmay and Prinz, 2011). Indeed, physical coupling between TPCs and ryanodine receptors at putative lysosome-ER junctions might well harmonize conflicting views regarding NAADP action (Patel et al., 2010; Patel and Brailoiu, 2012). 'Trigger zones' as sites of NAADP action have been proposed but ultra-structural evidence is scant (Kinnear et al., 2004; Patel and Brailoiu, 2012).

In the present study, we recapitulate complex $Ca^{2+}$ signals in human fibroblasts upon direct lysosomal permeabilisation in the absence of overt cellular stimulation. We also provide electron microscopic evidence for the existence of extensive membrane contacts between lysosomes and the ER. Our data provide new insight into cross-talk between $Ca^{2+}$ stores associated with acidic organelles and the ER.

## Results and Discussion

To probe the relationship between lysosomal and ER $Ca^{2+}$ stores, we used primary cultured human fibroblasts. These cells are large (~120 μm) and flat thus facilitate imaging. As shown in Fig. 1A, immunocytochemical analysis using a primary antibody raised to LAMP-1, revealed well resolved structures that were distributed throughout the cell. A similar distribution was obtained when live cells were incubated with Lysotracker Red, a fluorescent weak base that accumulates in acidic organelles (Fig. 1B). Addition of the lysosomotropic agent GPN resulted in a prompt loss of Lysotracker Red fluorescence consistent with the labelling of lysosomes (Fig. 1B). To quantify lysosomal $Ca^{2+}$ content, we monitored cytosolic $Ca^{2+}$ concentration in response to acute addition of GPN using cells loaded with the $Ca^{2+}$ sensitive indicator fura-2. Surprisingly, despite rapid permeabilisation of lysosomes, GPN evoked long-lasting $Ca^{2+}$ signals that persisted up to 15 min (Fig. 1C). Parallel measurements of Lysotracker Red fluorescence confirmed that GPN abolished Lysotracker Red fluorescence within ~3 min of addition under these conditions (Fig. 1D). Removal of extracellular $Ca^{2+}$ had little effect on $Ca^{2+}$ signals evoked by GPN indicating that $Ca^{2+}$ influx does not contribute significantly to GPN responses (Fig. 1E). For comparison, the effect of the SERCA pump inhibitor, thapsigargin, was used to estimate ER $Ca^{2+}$ content (Fig. 1F). GPN thus evokes relatively large cytosolic $Ca^{2+}$ signals that outlast lysosome integrity.

The kinetic mismatch between lysosome permeabilisation and cytosolic $Ca^{2+}$ responses was further characterised by simultaneous measurements of fura-2 and Lysotracker Red fluorescence at the single cell level (Fig. 2A-C). In all 36 coloaded cells examined ($n = 3$), we noted a primary linear increase in $Ca^{2+}$ upon GPN stimulation which correlated with the decrease in Lysotracker Red fluorescence. We term this increase in cytosolic $Ca^{2+}$ concentration the 'pacemaker' response. This was followed by one of three secondary responses. In most cells, the rise in cytosolic $Ca^{2+}$ accelerated, resulting in a prominent $Ca^{2+}$ spike. These spikes either repeated resulting in a series of $Ca^{2+}$ oscillations (Fig. 2A) or were abortive (Fig. 2B). In the remainder of cells, cytosolic $Ca^{2+}$ levels continued to increase monotonically primarily peaking after complete loss of Lysotracker Red fluorescence (Fig. 2C). Thus, there was marked variation in the time to peak response upon

GPN stimulation. Similar results were obtained in the absence of Lysotracker Red. From all 15 experiments analysed (with and without Lysotracker Red), the proportion of oscillatory (Fig. 2A) and abortive cells (Fig. 2B) were 48±5% and 29±5%, respectively (total number of cells = 177). At the spatial level, secondary responses to GPN were non-uniform. In cells displaying repeated $Ca^{2+}$ spikes, the responses derived from a particular sub-cellular location and spread throughout the cell in wave-like manner. These responses either initiated at one-end of the cell (67±5%, $n = 15$; Fig. 2D) or in the cell periphery (33±5%, $n = 15$; Fig. 2E). In the latter case, the wave propagated in a centripetal fashion resembling the closing of an iris. In all 104 oscillatory cells examined, the waves repeatedly initiated from the same sub-cellular locale. Taken together, these data indicate that GPN-evoked $Ca^{2+}$ signals are biphasic comprising an initial pacemaker response, which is probably lysosome dependent and a secondary response displaying spatial heterogeneity that appears lysosome independent.

GPN-evoked $Ca^{2+}$ responses are highly reminiscent of those evoked by cell-surface agonists. We therefore examined the effect of the physiological agonist bradykinin, which mobilises intracellular $Ca^{2+}$ stores, on GPN responses. Bradykinin generated robust cytosolic $Ca^{2+}$ signals in $Ca^{2+}$-free media. Subsequent treatment with GPN induced largely monotonic responses (Fig. 3B). Thus, the proportion of cells displaying oscillations was 57±10% ($n = 5$, 74 cells) and 10±4% ($n = 4$, 60 cells) in the absence and presence of bradykinin, respectively (Fig. 3A,B). To probe the contribution of ER $Ca^{2+}$ stores to GPN-evoked $Ca^{2+}$ signals, cells were pre-treated with thapsigargin. As shown in Fig. 3C, GPN stimulation evoked only a transient response after thapsigargin treatment similar to bradykinin. Secondary responses were not observed in any of the 279 cells examined ($n = 17$). To define the role of inositol trisphosphate ($InsP_3$) receptors, cells were pre-treated with the $InsP_3$ receptor antagonist 2-aminoethoxydiphenyl borate (2-APB). 2-APB did not induce a $Ca^{2+}$ signal (Fig. 3D). However, in its presence, the secondary responses to GPN were again largely eliminated (11±8% of oscillatory cells, $n = 3$, 45 cells). In contrast, GPN evoked typical complex $Ca^{2+}$ signals upon blockade of ryanodine receptors by ryanodine pre-treatment (Fig. 3E; 63±13% oscillatory cells, $n = 3$, 45 cells). Prolonged GPN-evoked $Ca^{2+}$ signals thus require $InsP_3$ receptors likely on the ER but the possible contribution of Golgi-localised $InsP_3$ receptors (Pizzo et al., 2011) cannot be excluded.

The ER is known to form several inter-organellar contact sites important for both $Ca^{2+}$ and lipid dialogue (Toulmay and Prinz, 2011). But much less is known concerning contacts between the ER and acidic organelles. We and others recently described contact sites between endosomes/multi-vesicular bodies (MVBs) and the ER (Eden et al., 2010; Rocha et al., 2009). As shown in Fig. 4, membrane contact sites (regions of close apposition of ~20 nm) were clearly visible between lysosomes and the ER. Quantification in random sections revealed that 82±2% of 140 lysosomes analysed form contact sites with the ER ($n = 3$). This is probably an underestimate, as lysosomes have a diameter of 200–500 nm and thus will extend over a number of experimental sections (70 nm thick) where additional contacts in different planes may have been missed. That such a large proportion of lysosomes display contacts in random sections indicates extensive physical coupling between lysosomes and the ER. Thus, a considerable fraction of the perimeter membrane of each lysosome is coupled. Consistent with our previous observations on ER–MVB contact sites, regions

where fibres appear to connect opposing ER and lysosome membranes (Fig. 4A, white arrows) were visible. The fibres resemble the tethers described within ER–mitochondria membrane contact sites (Csordás et al., 2006). Additionally, we identify areas where the apposing membranes appear to make direct contact with no discernible space between them (Fig. 4B, arrowhead).

To conclude, we functionally dissect GPN-evoked $Ca^{2+}$ signals into lysosomal and ER-derived components. Mobilisation of lysosomal $Ca^{2+}$ is thus sufficient to evoke complex $Ca^{2+}$ signals. These data provide direct support for the trigger hypothesis for NAADP action whereby physiological activation of endolysosomal $Ca^{2+}$ channels is proposed to trigger secondary $Ca^{2+}$ release via ER $Ca^{2+}$ channels (Cancela et al., 1999). In our experiments, potential confounding effects of NAADP on ER channels are circumvented. We also demonstrate that the majority of lysosomes make contact with the ER via extensive membrane contact sites which likely represent an important site for the triggering of complex $Ca^{2+}$ signals through juxtaposition of trigger and amplification $Ca^{2+}$ channels (Fig. 4C). The tethered contacts we identify would facilitate CICR between TPCs and ER $Ca^{2+}$ release channels (Fig. 4C, left). This is similar to the physical and functional arrangement of voltage-gated $Ca^{2+}$ channels and ryanodine receptors at diadic junctions of cardiac muscle (Protasi, 2002). More direct contacts provide a basis for potential protein-protein interactions between $Ca^{2+}$ release channels (Fig. 4C, right). This echoes the architecture of the excitation-contraction machinery in skeletal muscle (Protasi, 2002). Further ultra-structural and molecular definition of these novel membrane contact sites is warranted.

## Materials and Methods

### Cell culture

Human skin fibroblasts established from healthy females were maintained in DMEM supplemented with 10% v/v fetal bovine serum, 100 units/ml penicillin and 100 μg/ml streptomycin (all from Invitrogen) at 37 °C in a humidified atmosphere with 5% $CO_2$. Cells were plated on glass coverslips before experimentation.

### Immunocytochemistry

Fibroblasts were fixed for 10 min with 4% w/v paraformaldehyde, washed three times in phosphate-buffered saline (PBS) and then permeabilised for 5 min with 40 μM β-escin. Cells were washed again (three times in PBS), and blocked for 1 h with PBS supplemented with 1% w/v BSA and 10% v/v fetal bovine serum. Fibroblasts were sequentially incubated for 1 h at 37 °C with a primary anti-LAMP-1 (lysosomal-associated membrane protein 1) mouse antibody (1:100 dilution; H4A3 clone from Developmental Hybridoma Bank) and a secondary mouse antibody conjugated to Alexa Fluor 647 (1:100 dilution; Invitrogen) in blocking solution. Nuclei were labelled for 5 min with 1 μg/ml DAPI (4′, 6-diamidino-2-phenylindole). Cells were washed three times in PBS containing 0.1% v/v Tween in between incubations and mounted onto microscope slides with DABCO (1,4-diazabicyclo[2,2,2]octane).

### Live-cell imaging

Experiments were performed in HEPES-buffered saline (HBS) comprising (in mM) 1.25 $KH_2PO_4$, 2 $CaCl_2$, 2 $MgSO_4$, 3 KCl, 156 NaCl, 10 glucose and 10 HEPES (pH 7.4; all from Sigma). For measurement of cytosolic $Ca^{2+}$ concentration, fibroblasts were incubated with Fura-2AM (2.5 μM) and 0.005% v/v pluronic acid (from Invitrogen) for 1 h. For measurement of lysosome distribution/integrity, fibroblasts were incubated with 100 nM Lysotracker Red (Invitrogen) for 30 min. Cells were stimulated with 200 μM GPN (Santa Cruz Biotech), 10 nM bradykinin (Sigma), 1 μM thapsigargin, 100 μM 2-APB (2-aminoethoxydiphenyl borate) and 100 μM ryanodine (all sourced from Merck). Where indicated, $Ca^{2+}$ in HBS was replaced with 1 mM EGTA (Sigma).

### Epifluorescence microscopy

Epifluorescence images were captured every 3–8 s with a cooled coupled device camera (TILL Photonics) attached to an Olympus IX71 inverted fluorescence microscope fitted with a 20× objective, and a monochromator light source. Fura-2 and Lysotracker Red were excited at 340/380 nm and 560 nm and emitted fluorescence was captured using a 440 nm long pass filter and 590 nm filter, respectively.

### Confocal microscopy

Confocal images were captured using an LSM510 confocal scanner (Zeiss) attached to a Zeiss Axiovert 200 M inverted microscope fitted with a 63× Plan Apochromat water-immersion objective. DAPI, Lysotracker Red and Alexa Fluor 647 were excited at 364 nm, 560 nm and 633 nm and emitted fluorescence was captured using long pass 385 nm, 560–615 nm band pass or 655–719 nm band pass filters, respectively.

### Electron microscopy

BSA-gold was prepared by coupling 5 nm colloidal gold (BBI) to BSA as described previously (Slot and Geuze, 1985). Fibroblasts cultured on thermanox coverslips (Agar Scientific) were pulsed for 15 min with either BSA-gold or horseradish peroxidase (Sigma) and chased for 3 h in complete medium. This procedure labels exclusively lysosomes, as shown by their degradative capacity and LAMP-1 content (Futter et al., 1996). Cells were fixed and processed for electron microscopy essentially as described (Tomas et al., 2004) except that uranyl acetate (1%, 40 min incubation) was used in place of tannic acid, and samples were embedded in TAAB 812 hard formulation resin. Samples were viewed on a JEOL 1010 TEM and images acquired by a Gatan Orius SC100B charge-coupled device camera. Contact sites between lysosome and ER membranes were defined as regions of close apposition (~20 nm).

## Acknowledgments

We thank Tim Levine and Chi Li for useful discussions.

**Funding:** This was supported by the Biotechnology and Biological Sciences Research Council [grant number BB/K000942/1 to S.P.], Parkinson's UK [grant number K-1107 to S.P. and A.H.S.] and an IMPACT studentship from University College London [to B.S.K.].

## References


Berridge MJ. The endoplasmic reticulum: a multifunctional signaling organelle. Cell Calcium. 2002; 32:235–249. [PubMed: 12543086]

Berridge MJ, Lipp P, Bootman MD. The versatility and universality of calcium signalling. Nat. Rev. Mol. Cell Biol. 2000; 1:11–21. [PubMed: 11413485]

Brailoiu E, Churamani D, Pandey V, Brailoiu GC, Tuluc F, Patel S, Dun NJ. Messenger-specific role for nicotinic acid adenine dinucleotide phosphate in neuronal differentiation. J. Biol. Chem. 2006; 281:15923–15928. [PubMed: 16595650]

Brailoiu E, Churamani D, Cai X, Schrlau MG, Brailoiu GC, Gao X, Hooper R, Boulware MJ, Dun NJ, Marchant JS, et al. Essential requirement for two-pore channel 1 in NAADP-mediated calcium signaling. J. Cell Biol. 2009; 186:201–209. [PubMed: 19620632]

Brailoiu E, Rahman T, Churamani D, Prole DL, Brailoiu GC, Hooper R, Taylor CW, Patel S. An NAADP-gated two-pore channel targeted to the plasma membrane uncouples triggering from amplifying $Ca^{2+}$ signals. J. Biol. Chem. 2010; 285:38511–38516. [PubMed: 20880839]

Calcraft PJ, Ruas M, Pan Z, Cheng X, Arredouani A, Hao X, Tang J, Rietdorf K, Teboul L, Chuang KT, et al. NAADP mobilizes calcium from acidic organelles through two-pore channels. Nature. 2009; 459:596–600. [PubMed: 19387438]

Cancela JM, Churchill GC, Galione A. Coordination of agonist-induced $Ca^{2+}$-signalling patterns by NAADP in pancreatic acinar cells. Nature. 1999; 398:74–76. [PubMed: 10078532]

Churchill GC, Galione A. NAADP induces $Ca^{2+}$ oscillations via a two-pool mechanism by priming $IP_3$- and cADPr-sensitive $Ca^{2+}$ stores. EMBO J. 2001; 20:2666–2671. [PubMed: 11387201]

Churchill GC, Okada Y, Thomas JM, Genazzani AA, Patel S, Galione A. NAADP mobilizes $Ca^{2+}$ from reserve granules, lysosome-related organelles, in sea urchin eggs. Cell. 2002; 111:703–708. [PubMed: 12464181]

Coen K, Flannagan RS, Baron S, Carraro-Lacroix LR, Wang D, Vermeire W, Michiels C, Munck S, Baert V, Sugita S, et al. Lysosomal calcium homeostasis defects, not proton pump defects, cause endo-lysosomal dysfunction in PSEN-deficient cells. J. Cell Biol. 2012; 198:23–35. [PubMed: 22753898]

Csordás G, Renken C, Várnai P, Walter L, Weaver D, Buttle KF, Balla T, Mannella CA, Hajnóczky G. Structural and functional features and significance of the physical linkage between ER and mitochondria. J. Cell Biol. 2006; 174:915–921. [PubMed: 16982799]

Dammermann W, Zhang B, Nebel M, Cordiglieri C, Odoardi F, Kirchberger T, Kawakami N, Dowden J, Schmid F, Dornmair K, et al. NAADP-mediated $Ca^{2+}$ signaling via type 1 ryanodine receptor in T cells revealed by a synthetic NAADP antagonist. Proc. Natl. Acad. Sci. USA. 2009; 106:10678–10683. [PubMed: 19541638]

Eden ER, White IJ, Tsapara A, Futter CE. Membrane contacts between endosomes and ER provide sites for PTP1B-epidermal growth factor receptor interaction. Nat. Cell Biol. 2010; 12:267–272. [PubMed: 20118922]

Futter CE, Pearse A, Hewlett LJ, Hopkins CR. Multivesicular endosomes containing internalized EGF-EGF receptor complexes mature and then fuse directly with lysosomes. J. Cell Biol. 1996; 132:1011–1023. [PubMed: 8601581]

Galione A, Morgan AJ, Arredouani A, Davis LC, Rietdorf K, Ruas M, Parrington J. NAADP as an intracellular messenger regulating lysosomal calcium-release channels. Biochem. Soc. Trans. 2010; 38:1424–1431. [PubMed: 21118101]

Gerasimenko JV, Maruyama Y, Yano K, Dolman NJ, Tepikin AV, Petersen OH, Gerasimenko OV. NAADP mobilizes $Ca^{2+}$ from a thapsigargin-sensitive store in the nuclear envelope by activating ryanodine receptors. J. Cell Biol. 2003; 163:271–282. [PubMed: 14568993]

Gerasimenko JV, Lur G, Sherwood MW, Ebisui E, Tepikin AV, Mikoshiba K, Gerasimenko OV, Petersen OH. Pancreatic protease activation by alcohol metabolite depends on $Ca^{2+}$ release via acid store $IP_3$ receptors. Proc. Natl. Acad. Sci. USA. 2009; 106:10758–10763. [PubMed: 19528657]

Guse AH. Linking NAADP to ion channel activity: a unifying hypothesis. Sci. Signal. 2012; 5:pe18. [PubMed: 22534131]

Guse AH, Lee HC. NAADP: a universal $Ca^{2+}$ trigger. Sci. Signal. 2008; 1:re10. [PubMed: 18984909]

Hamilton SL, Serysheva II. Ryanodine receptor structure: progress and challenges. J. Biol. Chem. 2009; 284:4047–4051. [PubMed: 18927076]

Hohenegger M, Suko J, Gscheidlinger R, Drobny H, Zidar A. Nicotinic acid-adenine dinucleotide phosphate activates the skeletal muscle ryanodine receptor. Biochem. J. 2002; 367:423–431. [PubMed: 12102654]

Jadot M, Colmant C, Wattiaux-De Coninck S, Wattiaux R. Intralysosomal hydrolysis of glycyl-L-phenylalanine 2-naphthylamide. Biochem. J. 1984; 219:965–970. [PubMed: 6743255]

Kinnear NP, Boittin FX, Thomas JM, Galione A, Evans AM. Lysosome-sarcoplasmic reticulum junctions. A trigger zone for calcium signaling by nicotinic acid adenine dinucleotide phosphate and endothelin-1. J. Biol. Chem. 2004; 279:54319–54326. [PubMed: 15331591]

Lin-Moshier Y, Walseth TF, Churamani D, Davidson SM, Slama JT, Hooper R, Brailoiu E, Patel S, Marchant JS. Photoaffinity labeling of nicotinic acid adenine dinucleotide phosphate (NAADP) targets in mammalian cells. J. Biol. Chem. 2012; 287:2296–2307. [PubMed: 22117075]

Lloyd-Evans E, Morgan AJ, He X, Smith DA, Elliot-Smith E, Sillence DJ, Churchill GC, Schuchman EH, Galione A, Platt FM. Niemann-Pick disease type C1 is a sphingosine storage disease that causes deregulation of lysosomal calcium. Nat. Med. 2008; 14:1247–1255. [PubMed: 18953351]

Ludtke SJ, Tran TP, Ngo QT, Moiseenkova-Bell VY, Chiu W, Serysheva II. Flexible architecture of IP3R1 by Cryo-EM. Structure. 2011; 19:1192–1199. [PubMed: 21827954]

Luzio JP, Bright NA, Pryor PR. The role of calcium and other ions in sorting and delivery in the late endocytic pathway. Biochem. Soc. Trans. 2007; 35:1088–1091. [PubMed: 17956286]

Marchant JS, Lin-Moshier Y, Walseth TF, Patel S. The Molecular Basis for $Ca^{2+}$ Signalling by NAADP: Two-Pore Channels in a Complex? Messenger. 2012; 1:63–76. [PubMed: 25309835]

Patel S, Brailoiu E. Triggering of $Ca^{2+}$ signals by NAADP-gated two-pore channels: a role for membrane contact sites? Biochem. Soc. Trans. 2012; 40:153–157. [PubMed: 22260682]

Patel S, Docampo R. Acidic calcium stores open for business: expanding the potential for intracellular $Ca^{2+}$ signaling. Trends Cell Biol. 2010; 20:277–286. [PubMed: 20303271]

Patel S, Churchill GC, Galione A. Coordination of $Ca^{2+}$ signalling by NAADP. Trends Biochem. Sci. 2001; 26:482–489. [PubMed: 11504624]

Patel S, Marchant JS, Brailoiu E. Two-pore channels: Regulation by NAADP and customized roles in triggering calcium signals. Cell Calcium. 2010; 47:480–490. [PubMed: 20621760]

Pizzo P, Lissandron V, Capitanio P, Pozzan T. $Ca^{2+}$ signalling in the Golgi apparatus. Cell Calcium. 2011; 50:184–192. [PubMed: 21316101]

Protasi F. Structural interaction between RYRs and DHPRs in calcium release units of cardiac and skeletal muscle cells. Front. Biosci. 2002; 7:d650–d658. [PubMed: 11861217]

Pryor PR, Mullock BM, Bright NA, Gray SR, Luzio JP. The role of intraorganellar $Ca(^{2+})$ in late endosome-lysosome heterotypic fusion and in the reformation of lysosomes from hybrid organelles. J. Cell Biol. 2000; 149:1053–1062. [PubMed: 10831609]

Rizzuto R, Duchen MR, Pozzan T. Flirting in little space: the ER/mitochondria $Ca^{2+}$ liaison. Sci. STKE. 2004; 2004:re1. [PubMed: 14722345]

Rocha N, Kuijl C, van der Kant R, Janssen L, Houben D, Janssen H, Zwart W, Neefjes J. Cholesterol sensor ORP1L contacts the ER protein VAP to control Rab7-RILP-p150 Glued and late endosome positioning. J. Cell Biol. 2009; 185:1209–1225. [PubMed: 19564404]

Serysheva II, Ludtke SJ, Baker MR, Chiu W, Hamilton SL. Structure of the voltage-gated L-type $Ca^{2+}$ channel by electron cryomicroscopy. Proc. Natl. Acad. Sci. USA. 2002; 99:10370–10375. [PubMed: 12149473]

Shen D, Wang X, Li X, Zhang X, Yao Z, Dibble S, Dong XP, Yu T, Lieberman AP, Showalter HD, et al. Lipid storage disorders block lysosomal trafficking by inhibiting a TRP channel and lysosomal calcium release. Nat. Commun. 2012; 3:731. [PubMed: 22415822]

Slot JW, Geuze HJ. A new method of preparing gold probes for multiple-labeling cytochemistry. Eur. J. Cell Biol. 1985; 38:87–93. [PubMed: 4029177]

Tomas A, Futter C, Moss SE. Annexin 11 is required for midbody formation and completion of the terminal phase of cytokinesis. J. Cell Biol. 2004; 165:813–822. [PubMed: 15197175]

Toulmay A, Prinz WA. Lipid transfer and signaling at organelle contact sites: the tip of the iceberg. Curr. Opin. Cell Biol. 2011; 23:458–463. [PubMed: 21555211]

Yamaguchi S, Jha A, Li Q, Soyombo AA, Dickinson GD, Churamani D, Brailoiu E, Patel S, Muallem S. Transient receptor potential mucolipin 1 (TRPML1) and two-pore channels are functionally independent organellar ion channels. J. Biol. Chem. 2011; 286:22934–22942. [PubMed: 21540176]

Yamasaki M, Masgrau R, Morgan AJ, Churchill GC, Patel S, Ashcroft SJH, Galione A. Organelle selection determines agonist-specific $Ca^{2+}$ signals in pancreatic acinar and beta cells. J. Biol. Chem. 2004; 279:7234–7240. [PubMed: 14660554]

Zong X, Schieder M, Cuny H, Fenske S, Gruner C, Rötzer K, Griesbeck O, Harz H, Biel M, Wahl-Schott C. The two-pore channel TPCN2 mediates NAADP-dependent $Ca(^{2+})$-release from lysosomal stores. Pflugers Arch. 2009; 458:891–899. [PubMed: 19557428]



Europe PMC Funders Author Manuscripts

Europe PMC Funders Author Manuscripts

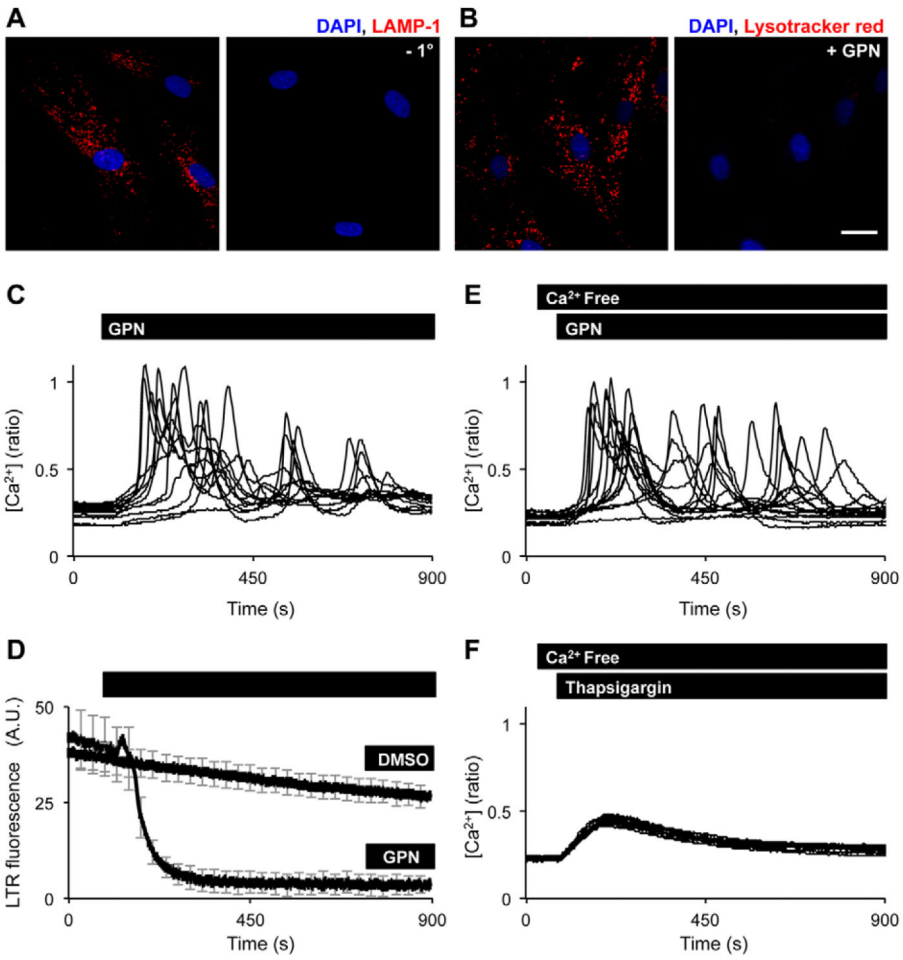


**Fig. 1. Osmotic permeabilisation of lysosomes evokes complex $Ca^{2+}$ signals**

(**A**) Confocal fluorescence image (red) of fibroblasts that were fixed and left unlabelled (right) or labelled (left) with a primary antibody raised to LAMP-1 and a far-red Alexa-Fluor-647-conjugated secondary antibody. (**B**) Confocal fluorescence images (red) of live fibroblasts that were labelled with Lysotracker Red before (left) or 216 seconds after (right) addition of 200 μM GPN. Nuclei were stained using DAPI (blue). Scale bar: 25 μm. (**C**,**D**) Single cell fluorescence responses recorded from cells loaded with either the $Ca^{2+}$ indicator fura-2 (C) or Lysotracker Red (D) and stimulated with 200 μM GPN or the vehicle (DMSO). (**E**,**F**) $Ca^{2+}$ signals in response to 200 μM GPN (E) or 1 μM thapsigargin (F) in the absence of extracellular $Ca^{2+}$.

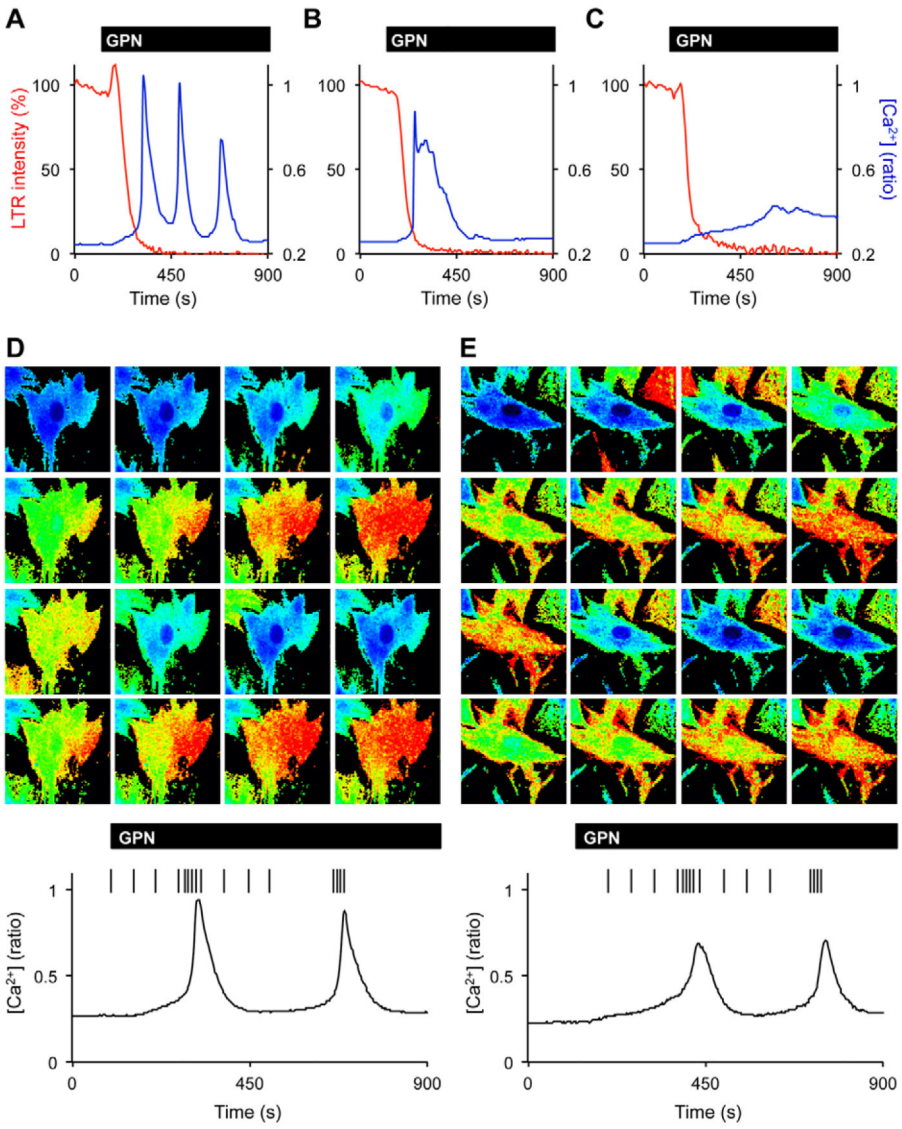


**Fig. 2. GPN-evoked $Ca^{2+}$ signals are spatiotemporally complex**

(**A-C**) Simultaneous measurement of fura-2 (blue line) and Lysotracker Red (LTR; red line) fluorescence from individual fibroblasts stimulated with 200 μM GPN in the absence of extracellular $Ca^{2+}$. Responses were grouped into three classes and representative examples of each are shown. (**D**,**E**) Pseudo-coloured images of GPN-evoked $Ca^{2+}$ increases (top left to bottom right). Representative responses showing $Ca^{2+}$ increases that propagated across the cell (D) or in a centripetal manner (E). The bottom traces are the temporal profiles from which spatial information was derived. Each vertical line (left to right) corresponds to an image above (top left to bottom right).

Europe PMC Funders Author Manuscripts

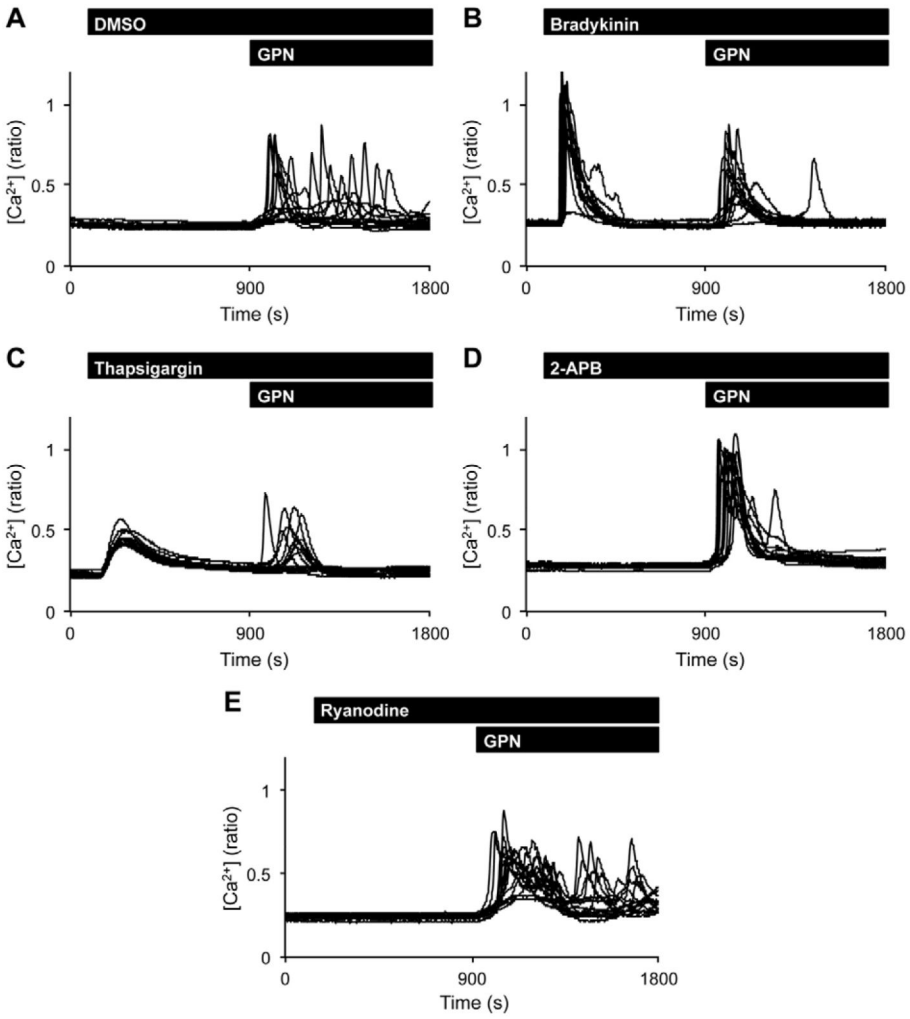


**Fig. 3. Prolonged GPN-evoked $Ca^{2+}$ signals derive from the ER**

$Ca^{2+}$ signals evoked by GPN (200 μM) in the absence of extracellular $Ca^{2+}$ following pre-treatment with vehicle (DMSO; **A**), 10 nM bradykinin (**B**), 1 μM thapsigargin (**C**), 100 μM 2-APB (**D**) or 100 μM ryanodine (**E**).

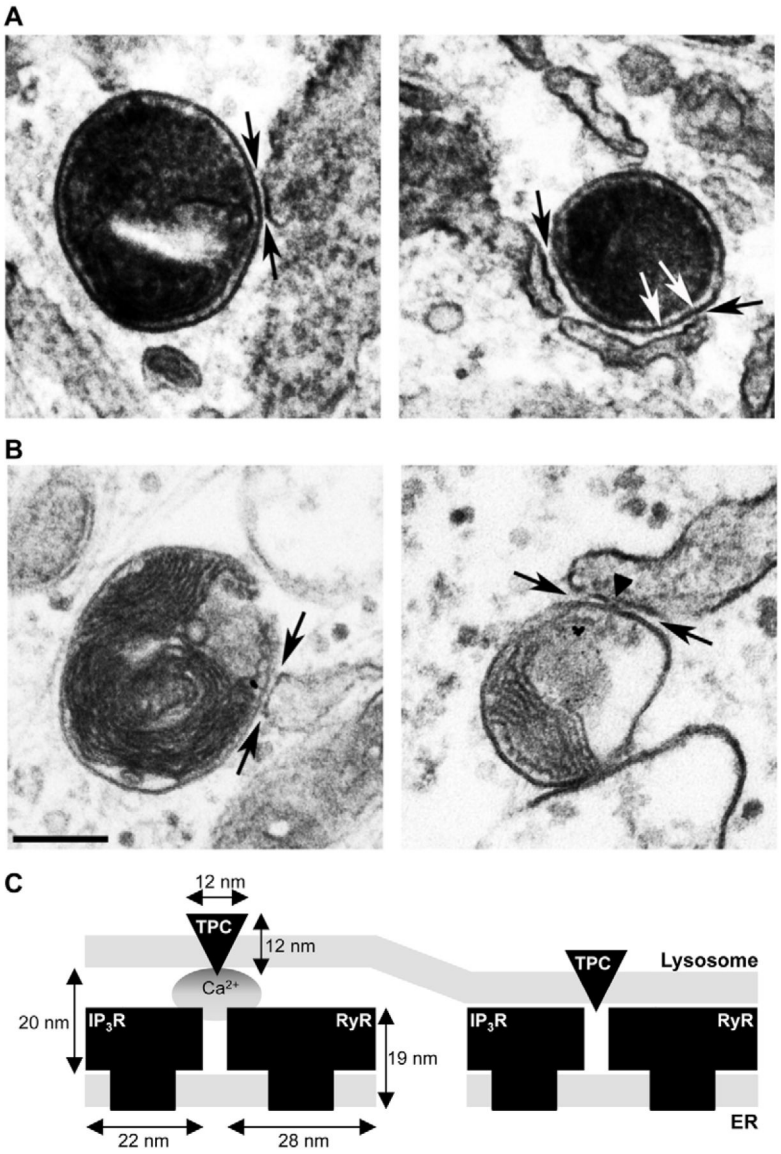


**Fig. 4. Lysosomes and ER form membrane contact sites**

(**A**,**B**) Electron micrographs of fibroblasts pulsed with horseradish peroxidase (A) or BSA-gold (B) to label lysosomes. Membrane contact sites between lysosomes and the ER are indicated by the black arrows. Fibres connecting opposing membranes (white arrows) and regions of very close membrane apposition (arrowhead) are marked. Scale bar: 200 nm. (**C**) Model showing juxtaposition of lysosomal TPCs (triangle) and ER inositol trisphosphate ($IP_3R$)/ryanodine (RyR) receptors (square shapes) at lysosome-ER membrane contact sites. TPCs have been shown to couple to both Ins$P_3$ (Calcraft et al., 2009) and RyR (Brailoiu et al., 2009). Lysosomes and ER may communicate through $Ca^{2+}$ released from TPCs (circle; left) or through more direct interaction (right) where apposing membranes are more closely positioned. Dimensions for the TPC were assumed to be similar to the skeletal muscle L-type $Ca^{2+}$ channel to which TPCs have sequence and topological similarity (Serysheva et

al., 2002). Dimensions for Ins$P_3$ and RyR were taken from Hamilton and Serysheva, and Ludtke et al. (Hamilton and Serysheva, 2009; Ludtke et al., 2011).



Europe PMC Funders Author Manuscripts